Scaling between stomatal size and density in forest plants

Congcong Liu[1,2#], Christopher D. Muir[3#], Ying Li[1], Li Xu[1], Mingxu Li[1], Jiahui Zhang[1,2], Hugo Jan de Boer[4], Lawren Sack[5], Xingguo Han[6], Guirui Yu[1,2], Nianpeng He[1,2,7*]

[1] Key Laboratory of Ecosystem Network Observation and Modeling, Institute of Geographic Sciences and Natural Resources Research, Chinese Academy of Sciences, Beijing 100101, China

[2] University of Chinese Academy of Sciences, Beijing 100049, China

[3] School of Life Sciences, University of Hawai'i at Mānoa, Honolulu, 96822, USA

[4] Copernicus Institute of Sustainable Development, Department of Environmental Sciences, Utrecht University, the Netherlands, 80125, Utrecht.

[5] Department of Ecology and Evolutionary Biology, University of California, Los Angeles, 90025, USA

[6] State Key Laboratory of Vegetation and Environmental Change, Institute of Botany, Chinese Academy of Sciences, Beijing 100093, China

[7] Institute of Grassland Science, Northeast Normal University, and Key Laboratory of Vegetation Ecology, Ministry of Education, Changchun 130024, China

[#] These authors contributed equally to this work.

*Corresponding author Nianpeng He (henp@igsnrr.ac.cn).

Tel.: +86-10-64889263

Fax: +86-10-64889399

The size and density of stomatal pores limit the maximum rate of leaf carbon gain and water loss (g_{max}) in land plants. Stomatal size and density are negatively correlated at broad phylogenetic scales, such that species with small stomata tend to have greater stomatal density, but the consequences of this relationship for leaf function has been controversial. The prevailing hypothesis posits that the negative scaling of size and density arises because species that evolved higher g_{max} also achieved reduced allocation of epidermal area to stomata (stomatal-area minimization). Alternatively, the negative scaling of size and density might reflect the maintenance of a stable mean and variance in g_{max} despite variation in stomatal size and density, which would result in a higher allocation of epidermal area to achieve high g_{max} (stomatal-area increase). Here, we tested these hypotheses by comparing their predictions for the structure of the covariance of stomatal size and density across species, applying macroevolutionary models and phylogenetic regression to data for 2408 species of angiosperms, gymnosperms, and ferns from forests worldwide. The observed stomatal size-density scaling and covariance supported the stomatal area increase hypothesis for high g_{max}. Thus, contrary to the prevailing view, higher g_{max} is not achieved while minimizing stomatal area allocation but requires increasing epidermal area allocated to stomata. Understanding of optimal stomatal conductance, photosynthesis, and plant water-use efficiency used in Earth System and crop productivity models will thus be improved by including the cost of higher g_{max} both in construction cost of stomata and opportunity cost in epidermal space.

45 Stomatal pores are critical determinants of the function of plants and the composition of
46 the atmosphere [1]. The stomatal conductance to diffusion of water vapor and CO_2 (g_s) influences a
47 broad spectrum of ecological processes at leaf, community, and ecosystem scales, including
48 photosynthesis, net primary production, and water use efficiency [2,3]. Theoretically, stomata can
49 regulate g_s through evolutionary or plastic shifts in stomatal size or numbers [4] or through short-
50 term stomatal aperture changes [5]. The g_s, and its typical operational value (g_{op}), can thus vary
51 from near zero with stomata fully closed and g_{max} with stomata fully open. However, g_{op} and g_{max}
52 are correlated across plants measured under controlled conditions [6,7], possibly to maintain the
53 ratio g_{op}:g_{max} in which stomatal pore aperture is most responsive to guard cell turgor pressure [8].
54 There has been substantial debate about whether to increase g_{max}, plants must allocate a greater
55 fraction of limited epidermal area to stomata, which might be costly. Stomatal optimization used
56 to predict water use, productivity, and drought responses in critical global vegetation and crop
57 models could be sensitive to costs of stomata, but they are rarely included[9]. Because of their
58 importance in controlling leaf water and CO_2 fluxes, stomatal anatomy could be integrated with
59 other plant traits to inform global vegetation and crop models [10-13] if we better understood what
60 drives variation in these traits. Indeed, the anatomical traits stomatal density (D_s, number of
61 pores per unit epidermal area) and size (A_s, area of guard cells surrounding each pore) have been
62 widely used to study the adaptation and competition of plants because they are reliable indicators
63 of g_{max} to water vapor and CO_2 [14-20]. Yet, while the covariation of stomatal size and density
64 within and across species has emerged as a critical constraint on g_{max} in controlled experiments
65 and specific ecosystems [21,22], these traits have engendered controversy when considering the
66 diversity of species in natural vegetation at regional or global scales.
67

Variation in stomatal size and density may be constrained to minimize leaf surface area (stomatal-area minimization) or leaves may allocate more area to increase stomatal conductance (stomatal-area increase). We adjudicate between these competing hypotheses by considering how they affect stomatal trait covariance differently and test competing predictions with a global data set of stomatal anatomy in forest plants. A leaf's g_{max} is determined by stomatal anatomy:

$$g_{max} = bmD_S A_S^{0.5}, \quad (1)$$

where b and m are biophysical and morphological constants, respectively [23] (see Methods for equations to calculate these constants). The fraction of epidermal area allocated to stomata (f_s) is a fundamental physical constraint on g_{max} because f_S cannot exceed unity, and

$$f_S = D_S A_S, \quad (2)$$

Therefore, D_S and A_S define both g_{max} and f_S, two related traits that affect gas exchange, productivity, and fitness.

Stomatal size and density covary negatively across species, reducing the variation in g_{max} and f_S compared to what it would be if these anatomical traits were uncorrelated[4,22–27]. Despite that the inverse relationship between stomatal size and density has been recognized since 1865 [24], its evolutionary origin and its consequences have not been understood. The leading view, established by Franks and Beerling [25], is that the size-density relationship arises due to the minimization of the area of epidermis allocated to stomata, such that the evolution of more stomata involves the reduction of stomatal size. By Eq. 2, a higher g_{max} can be achieved with a smaller total stomatal area by increasing stomatal number and reducing stomatal size, because smaller stomata also have a shorter channel for diffusion. Thus, selection for higher g_{max} would result in more numerous, smaller stomata, to minimize epidermal allocation to stomata. However, this hypothesis, and its implications that epidermal allocation to stomata is minimized,

and can be strongly reduced, have not been tested. Such reduction of allocation would greatly reduce the construction and maintenance cost of guard cells, and also the opportunity cost in other epidermal leaf structures, and in light penetration to the mesophyll. A counter-hypothesis to the 'stomatal-area minimization' is the 'stomatal-area increase' hypothesis in which selection for higher g_{max} would lead to greater surface allocation, and thus incur substantial cost (Fig. 1). It is critical to determine which of these hypotheses is consistent with the observed stomatal size-density relationship. An implication of stomatal-area minimization is that extremely high f_S is rare because of costs associated with allocating too much epidermal area to stomata[27–32], and g_{max} is ultimately constrained by the costs of high f_S. By contrast, an implication of the stomatal-area increase hypothesis is that on average high g_{max} incur major costs in stomatal volume construction cost and in epidermal space.

Both the stomatal-area minimization and stomatal increase hypotheses for high g_{max} would be consistent with an inverse stomatal size-density relationship. We developed theory showing that the scaling exponents of the relationship would differ between the hypotheses using a new, additional criterion based on models of macroevolutionary landscapes [26-29] originally derived from quantitative genetics. Over macroevolutionary time, variation in phenotypic traits is usually constrained by some combination of physical, developmental, or ecological factors. Theoretically, this process can be described by an Ornstein-Uhlenbeck (OU) model in which trait variation expands through time until it reaches a stationary distribution around a long-term average[27]. In macroevolutionary models, the OU process describes the movement of the adaptive optima itself. Species should be close to their current adaptive optimum if there is sufficient genetic variation, so phenotypic constraint is caused by limits on movement in the adaptive optima, not limits on response to selection.

We propose that scaling between stomatal size and density does not reflect constraints on either trait alone, but rather the constraint on a composite trait associated with stomatal size and density. That is, if the composite traits f_S and/or g_{max} were constrained following an OU process then constituent traits (size and density) should *appear to evolve* as if they are mutually constrained. This prediction is based on quantitative genetic theory which shows that a constraint on composite traits imposed by stabilizing selection limits variation in constituent traits[30]. We tested whether the observed size-density scaling across 2408 species was consistent with a stronger constraint on f_S or g_{max}. Note that both f_S and g_{max} equations have the form:

$$\boldsymbol{Z_S = \lambda D_S A_S^{\beta}}, \tag{3}$$

where is Z_S is a composite stomatal trait that is proportional to the product of constituent traits, stomatal density and stomatal size with scaling exponent β multiplied by a scalar λ. For g_{max}, $\lambda = bm$ and $\beta = 0.5$ (Eq. 1); for f_S, $\lambda = 1$ and $\beta = 1$ (Eq. 2). Next, we linearize Eq. 3 by log-transformation:

$$\boldsymbol{z_S = \log(\lambda) + d_S + \beta a_S}. \tag{4}$$

Lowercase variables are the log-transformed versions of their uppercase counterparts. Log-transformation is also desirable here because D_S and A_S are log-normally distributed[27]. Using random variable algebra, the variance in z_S is defined as:

$$\mathrm{Var}(\boldsymbol{z_S}) = \mathrm{Var}(\boldsymbol{d_S}) + \boldsymbol{\beta^2}\mathrm{Var}(\boldsymbol{a_S}) + \boldsymbol{2\beta}\mathrm{Cov}(\boldsymbol{d_S, a_S}). \tag{5}$$

The scaling exponent β minimizes $\mathrm{Var}(z_S)$, the most constrained composite trait, is:

$$\boldsymbol{\beta = -\frac{Cov(d_S, a_S)}{Var(d_S)}} \tag{6}$$

The right-hand side of this equation is the negative of the ordinary linear regression slope of log-stomatal size against log-density, which means that β can be estimated using regression methods, but a negative relationship will result in positive value of β. The stomatal-area

minimization hypothesis predicts that $\hat{\beta} = 1$ whereas the stomatal-area increase hypothesis predicts that $\hat{\beta} = 0.5$. Forward-time, individual based, macroevolutionary quantitative genetic simulations confirm that these predictions hold true regardless of underlying assumptions about mutational and genetic variance (Supplementary Information).

We estimated stomatal size-density scaling in 2408 forest plant specues from new field-collected samples over 28 sites in China and global synthesis of data from the literature (Fig. 2) and estimated the scaling exponent β using OU phylogenetic multiple regression with group (Angiosperm, Pteridophyte, Gymnosperm) and growth form (tree, shrub, herb) as covariates (see Methods)

Our analysis shows that stomatal size-density scaling among forest plant species is consistent with selection for higher g_{max} increasing stomatal area allocation, and not minimizing area allocation (Fig. 3). Given the variance in stomatal density, the covariance between size and density among forest species minimizes the variance in g_{max}. There is no evidence that scaling differs between major groups, Angiosperms, Gymnosperms, and Pteridophytes (Fig. 3a; Table S1), but g_{max} is 49% (17-88% 95% CI; $P = 0.001$) and 14% (1-30% 95% CI; $P = 0.04$) higher in Angiosperms than Gymnosperms and Pteridophytes, respectively (Table S2). Trees also have 18% (8-28% 95% CI; $P < 0.0001$) and 48% (39-59% 95% CI; $P < 0.0001$) greater g_{max} than shrubs and herbs, respectively (Table S2). The mean and variance in $\log(g_{max})$ are nearly invariant across latitude, temperature, and precipitation gradients, indicating that most of the variation in g_{max} occurs within rather than between forest sites (Fig. 4).

Our results overturn the prevailing view that size-density scaling results in minimized stomatal area allocation. Instead, we find that negative covariance between stomatal size and density is consistent with stomatal area allocation increasing with g_{max}, and, furthermore that

limits on the fraction of epidermis allocated to stomatal (f_S) are a secondary consequence of limits on g_{max}. Our results differ from previous studies because we adopted a new theoretical framework based on quantitative genetic and macroevolutionary theory. Previous analyses [31] estimated scaling exponents close to 1 for hypostomatous leaves using standardized major axis (SMA) regression, which finds the scaling exponent which minimizes residual variance in both d_S and a_S. SMA regression, adopted from allometry, does not enable analysis of how stomatal size-density scaling shapes covariance between constituent traits (see Supplementary Information). Although estimated scaling using standard phylogenetic regression approaches (see Methods), it is more appropriate to interpret the results not as minimizing residual variance, but rather estimating the β consistent with the covariance structure of stomatal size and density (Fig. 1).

Our results have at least three important implications for understanding the evolutionary consequences of the stomatal size-density scaling relationship. First, size-density scaling implies that extreme values of g_{max} do not provide competitive advantage across environments. Low g_{max} limits plants productivity by reducing the CO_2 supply for photosynthesis under favorable conditions. Excessively high g_{max} may be rare because selection on g_{max} most likely ensures a proper g_{op}:g_{max} ratio that situates leaf g_{op} in a region of maximal control to respond rapidly to changing environments [8]. High anatomical g_{max} may also increase the risk of hydraulic failure [32] especially under transient conditions, thereby setting a physical upper limit to leaf gas exchange. Other possible costs include interference of stomatal movements and diffusion, as well as energetic costs [31,33]. The scaling between size and density is consistent with excessive g_{max} incurring a major cost that cannot be obviated by stomatal area-minimization. Future work should prioritize identifying the fitness costs and evolutionary constraints that prevent higher

177 g_{max} from evolving. Second, if g_{max} is the primary constraint, this implies that plants could
178 allocate a greater fraction of their epidermal area to stomata than they currently do without
179 incurring a major cost. For example, we predict that if stomatal size and density could be
180 manipulated independently, anatomies with the same g_{max}, but different f_S, would have similar
181 fitness. Another important corollary is that smaller stomata were not directly required to increase
182 g_{max} in angiosperms. All three major land plant lineages have similar variance in g_{max} (Fig. 3b);
183 gymnosperms and pteridophytes have lower average g_{max} because they have on average a lower
184 d_S for a given a_S, not because of differences in the scaling relationship. Increased g_{op} may be an
185 indirect consequence of higher stomatal density being linked to increases in leaf water transport
186 capacity, for example, by decreasing the distance between vein and stomata, allowing stomata to
187 stay open[40]. The primary constraint on maximum stomatal conductance appears to be selection
188 itself, implying that vegetation and crop models should incorporate costs of extreme trait values
189 in their predictions.
190

Methods

Stomatal trait data from global forests

The stomatal dataset of global forests involved the information of a total of 2408 plant species from natural forests. The data consists of novel field data collected from Chinese forest communities and a compilation of published literature values.

Our field data were collected from 28 typical forest communities occurring between 18.7 °N and 53.3 °N latitude in China. The field sites were selected to cover most of the forest types in the northern hemisphere, including cold-temperate coniferous forest, temperate deciduous forest, subtropical evergreen forest, and tropical rain forest (Fig. 2). In total, we sampled 28 forest sites. We used the Worldclim database [34] to extract additional data on mean annual temperature (MAT) and precipitation (MAP) over the period 1960-1990 using latitude and longitude. Among these forests, mean annual temperature (MAT) ranged from -5.5-23.2 °C, and mean annual precipitation (MAP) varied from 320 to 2266 mm. The field investigation was conducted in July-August, during the peak period of growth for forests. Sampling plots were located within well-protected national nature reserves or long-term monitoring plots of field ecological stations, with relatively continuous vegetation. Four experimental plots (30 × 40 m) were established in each forest.

Leaves from trees, shrubs, and herbs were collected within and around each plot. For trees, mature leaves were collected from the top of the canopy in four healthy trees and mixed as a composite sample. Eight to 10 leaves from the pooled samples were cut into roughly 1.0 × 0.5 cm pieces along the main vein, and were fixed in formalin-aceto-alcohol (FAA) solution (5 ml 38 % formalin, 90 ml 75 % ethanol, 5 ml 100 % glacial acetic acid, and 5 ml 37 % methanol) [35].

In the laboratory, three small pieces were randomly sampled, and each replicate was photographed twice using a scanning electron microscopy (Hitachi SN-3400, Hitachi, Tokyo, Japan) on the lower surface at different positions. We focused on the lower epidermis [22], because a previous study has demonstrated that most of leaf upper epidermis has no stomata for forest plants [36].

In each photograph, the number of stomata was recorded, and D_S was calculated as the number of stomata per unit leaf area. Simultaneously, five typical stomata were selected to measure stomatal size using an electronic image analysis equipment (MIPS software, Optical Instrument Co. Ltd., Chongqing, China).

Peer-reviewed papers on leaf stomata were collected using an all-databases search of Web of Science (www.webofknowledge.com) from 1900 to 2018 using "forest" and "stomata" as a topic, in line with the principle of "nature forest, non-intervention, species name". There were a total of 90 papers (see Supporting Table S3) which met our requirements, yielding D_S and L measurements from 413 plant species (Fig. 2) from which we calculated g_{max} and f_S. f_S is proportional to the stomatal pore area index (SPI), which defined as the product of D_S and stomatal length (L) squared [37], because $A_S = mL^2$ [23].

We calculated g_{max} (Equation 1) to water vapor at a reference leaf temperature (T_{leaf} = 25° C) following Sack and Buckley [23]. They defined a biophysical and morphological constant as:

$$b = \frac{D_{wv}}{v}$$

$$m = \frac{\pi c^2}{j^{0.5}(4hj + \pi c)}$$

231 b is the diffusion coefficient of water vapor in air (D_{wv}) divided by the kinematic viscosity of
232 dry air (ν). $D_{wv} = 2.49 \times 10^{-5}$ m^2 s^{-1} and $\nu = 2.24 \times 10^{-2}$ m^3 mol^{-1} at 25°[38]. For kidney-
233 shaped guard cells, $c = h = j = 0.5$; for dumbbell-shaped guard cells in the Poaceae, $c = h =$
234 0.5 and $j = 0.125$. We used the species average g_{max} and f_S for all analyses.

235 *Phylogenetic regression*

236 By positing that the least variable composite of stomatal size and density indicates the trait
237 with the most constraint (Fig. 1), we identify a new way to estimate the scaling exponent β (Eq.
238 6) using linear regression estimates, but these estimates should still account for phylogenetic
239 nonindependence. We used the Plant List (http://www.theplantlist.org) to confirm species names,
240 then we assembled a synthetic phylogeny using S.PhyloMaker [39]. We fit phylogenetic regression
241 models using the **phylolm** version 2.6 package in R [40]. As we derived in the main text, the
242 scaling exponent β can be estimated from the slope of the regression of a_S on d_S, where $\hat{\beta} =$
243 $-$slope. We estimated separate scaling exponents for major groups, Angiosperms, Pteridophytes,
244 and Gymnosperms. We also estimated different intercepts, corresponding with different average
245 g_{max} values, for functional types (herbs, shrubs, and trees) and grasses, because of their unique
246 stomatal anatomy. We used the "OUrandomRoot" model of trait evolution. 95% confidence
247 intervals for all parameters were estimated from 1000 parametric bootstrap samples generated by
248 simulating from the best-fit model and re-fitting. *P*-values for coefficients are based on *t*-tests.
249 We used the same methods to test whether g_{max} (log-transformed for homoskedasticity) was
250 affected by |latitude|, MAP, MAT, group (Angiosperms, Pteridophytes, Gymnosperms), and/or
251 functional type (herb, shrub, tree). One gymnosperm species, *Torreya fargesii*, had substantially
252 lower stomatal size than would be predicted from its density (Fig. 3a). There results of the paper
253 did not change if this outlier was excluded because the confidence intervals for stomatal-density

scaling are very wide for Gymnosperms regardless. Therefore, we excluded this species from statistical analyses but show it in the figure for completeness. All data were analyzed in R [41]version 4.0.5

References

1 Berry, J. A., Beerling, D. J. & Franks, P. J. Stomata: key players in the earth system, past and present. *Curr. Opin. Plant Biol.* **13**, 232-239 (2010).

2 Cramer, W. *et al.* Global response of terrestrial ecosystem structure and function to CO_2 and climate change: results from six dynamic global vegetation models. *Glob. Change Biol.* **7**, 357-373 (2001).

3 Haworth, M., Elliott-Kingston, C. & McElwain, J. C. Stomatal control as a driver of plant evolution. *J. Exp. Bot.* **62**, 2419-2423 (2011).

4 Jordan, G. J., Carpenter, R. J., Koutoulis, A., Price, A. & Brodribb, T. J. Environmental adaptation in stomatal size independent of the effects of genome size. *New Phytol.* **205**, 608-617 (2015).

5 Hetherington, A. M. & Woodward, F. I. The role of stomata in sensing and driving environmental change. *Nature* **424**, 901-908 (2003).

6 Franks, P. J. *et al.* Sensitivity of plants to changing atmospheric CO_2 concentration: from the geological past to the next century. *New Phytol.* **197**, 1077-1094 (2013).

7 Haworth, M., Elliott-Kingston, C. & McElwain, J. C. Co-ordination of physiological and morphological responses of stomata to elevated CO_2 in vascular plants. *Oecologia* **171**, 71-82 (2013).

8 Franks, P. J., Leitch, I. J., Ruszala, E. M., Hetherington, A. M. & Beerling, D. J. Physiological framework for adaptation of stomata to CO_2 from glacial to future concentrations. *Philos. T. R. Soc. B.* **367**, 537-546 (2012).

9 Deans, R. M., Brodribb, T. J., Busch, F. A. & Farquhar, G. D. Optimization can provide the fundamental link between leaf photosynthesis, gas exchange and water relations. *Nat. Plants* **6**, 1116-1125 (2020).

10 Ordoñez, J. C. *et al.* A global study of relationships between leaf traits, climate and soil measures of nutrient fertility. *Glob. Ecol. Biogeogr.* **18**, 137-149 (2009).

11 Yuan, Z. Y. & Chen, H. Y. H. Global-scale patterns of nutrient resorption associated with latitude, temperature and precipitation. *Glob. Ecol. Biogeogr.* **18**, 11-18 (2009).

12 Díaz, S. *et al.* The global spectrum of plant form and function. *Nature* **529**, 167-171 (2016).

13 Freschet, G. T. *et al.* Climate, soil and plant functional types as drivers of global fine-root trait variation. *J. Ecol.* **105**, 1182-1196 (2017).

14 Brown, H. T. & Escombe, F. Static diffusion of gases and liquids in relation to the assimilation of carbon and translocation in plants. *Proc. R. Soc. Lond.* **67**, 124-128 (1901).

15 Parlange, J.-Y. & Waggoner, P. E. Stomatal dimensions and resistance to diffusion. *Plant Physiol.* **46**, 337-342 (1970).

16 Franks, P. J. & Farquhar, G. D. The effect of exogenous abscisic acid on stomatal development, stomatal mechanics, and leaf gas exchange in *Tradescantia virginiana*. *Plant Physiol.* **125**, 935-942 (2001).

17 Vatén, A. & Bergmann, D. C. Mechanisms of stomatal development: an evolutionary view. *EvoDevo* **3**, 11 (2012).

18 McElwain, J. C., Yiotis, C. & Lawson, T. Using modern plant trait relationships between observed and theoretical maximum stomatal conductance and vein density to examine patterns of plant macroevolution. *New Phytol.* **209**, 94-103 (2016).

19 Conesa, M. À., Muir, C. D., Molins, A. & Galmés, J. Stomatal anatomy coordinates leaf size with Rubisco kinetics in the Balearic *Limonium*. *AoB Plants* **12** (2019).

20 Murray, M. *et al.* Consistent relationship between field-measured stomatal conductance and theoretical maximum stomatal conductance in c3 woody angiosperms in four major biomes. *Int. J. Plant Sci.* **181**, 142-154 (2020).

21 Wang, R. *et al.* Latitudinal variation of leaf stomatal traits from species to community level in forests: linkage with ecosystem productivity. *Sci. Rep.* **5**, 14454 (2015).

22 Liu, C. *et al.* Variation of stomatal traits from cold temperate to tropical forests and association with water use efficiency. *Funct. Ecol.* **32**, 20-28 (2018).

23 Sack, L. & Buckley, T. N. The developmental basis of stomatal density and flux. *Plant Physiol.* **171**, 2358-2363 (2016).

24 Weiss, A. G. *Untersuchungen über die Zahlen-und Grössenverhältnisse der Spaltöffnungen.* Vol. 4 125-196 (Jahrbu¨cher fu¨r Wissenschaftliche Botanik, 1865).

25 Franks, P. J. & Beerling, D. J. Maximum leaf conductance driven by CO_2 effects on stomatal size and density over geologic time. *Proc. Natl. Acad. Sci. USA.* **106**, 10343-10347 (2009).

26 Pennell, M. W. & Harmon, L. J. An integrative view of phylogenetic comparative methods: connections to population genetics, community ecology, and paleobiology. *Ann N.Y. Acad. Sci.* **1289**, 90-105 (2013).

27 Hansen, T. F. Stabilizing selection and the comparative analysis of adaptation. *Evolution* **51**, 1341-1351 (1997).

28 Uyeda, J. C. & Harmon, L. J. A novel bayesian method for inferring and interpreting the dynamics of adaptive landscapes from phylogenetic comparative data. *Syst. Biol.* **63**, 902-918 (2014).

29 Boucher, F. C., Démery, V., Conti, E., Harmon, L. J. & Uyeda, J. A general model for estimating macroevolutionary landscapes. *Syst. Biol.* **67**, 304-319 (2017).

30 Walsh, B. & Blows, M. W. Abundant Genetic Variation + Strong Selection = Multivariate Genetic Constraints: A Geometric View of Adaptation. *Annu. Rev. Ecol. Evol. S.* **40**, 41-59 (2009).

31 de Boer, H. J. *et al.* Optimal allocation of leaf epidermal area for gas exchange. *New Phytol.* **210**, 1219-1228 (2016).

32 Henry, C. *et al.* A stomatal safety-efficiency trade-off constrains responses to leaf dehydration. *Nat. Commun.* **10**, 3398 (2019).

33 Farquhar, G. D., Cowan, I. R. & Zeiger, E. *Stomatal Function*. (Stanford University Press, 1987).

34 Hijmans, R. J., Cameron, S. E., Parra, J. L., Jones, P. G. & Jarvis, A. Very high resolution interpolated climate surfaces for global land areas. *Int. J. Climatol.* **25**, 1965-1978 (2005).

35 He, N. *et al.* Variation in leaf anatomical traits from tropical to cold-temperate forests and linkage to ecosystem functions. *Funct. Ecol.* **32**, 10-19 (2018).

36 Muir, C. D. Light and growth form interact to shape stomatal ratio among British angiosperms. *New Phytol.***218**, 242-252 (2018).

37 Sack, L., Cowan, P. D., Jaikumar, N. & Holbrook, N. M. The 'hydrology' of leaves: co-ordination of structure and function in temperate woody species. *Plant Cell Environ.* **26**, 1343-1356 (2003).

38 Monteith, J. L. & Unsworth, M. H. *Principles of environmental physics: plants, animals, and the atmosphere.* (Elsevier/Academic Press, 2013).

39 Qian, H. & Jin, Y. An updated megaphylogeny of plants, a tool for generating plant phylogenies and an analysis of phylogenetic community structure. *J. Plant Ecol.* **9**, 233-239 (2015).

40 Ho, L. & Ané, C. A linear-time algorithm for Gaussian and non-Gaussian trait evolution models. *Syst. Biol.* **63**, 397-408 (2014).

41 R Core Team. R: *A Language and Environment for Statistical Computing*. (R Foundation for Statistical Computing, 2019)

Acknowledgements

Financial support was supported by the National Natural Science Foundation of China (31988102, 42071303), the National Key R&D Program of China (2017YFA0604803), National Science and Technology Basic Resources Survey Program of China (2019FY101300) , US National Science Foundation 1929167 (to CDM), and the Project funded by China Postdoctoral Science Foundation (2020M680663). We thank "Functional Trait Database of Terrestrial Ecosystems in China (China_Trait)" for sharing data, further information for other materials should contact to N.P. He (henp@igsnrr.ac.cn). There are no conflicts of interest to declare.

Author contributions

N.H. and G.Y. designed field sampling; N.H., C.D.M, and C.L. conceived the initial ideas; C.L., N.H., Y.L. J.Z., M.L. and L.X collected the data; C.L. writed the first draft, and C.D.M. made major revision on it, and C.D.M. contributed the final mathematical derivations, data analysis, and wrote the final manuscript; L.S., H.J.B., C.L., N.H., G.Y., and X.H. revised the manuscript. All authors gave final approval for publication.

392 **Supplementary information**

393 **Figures**

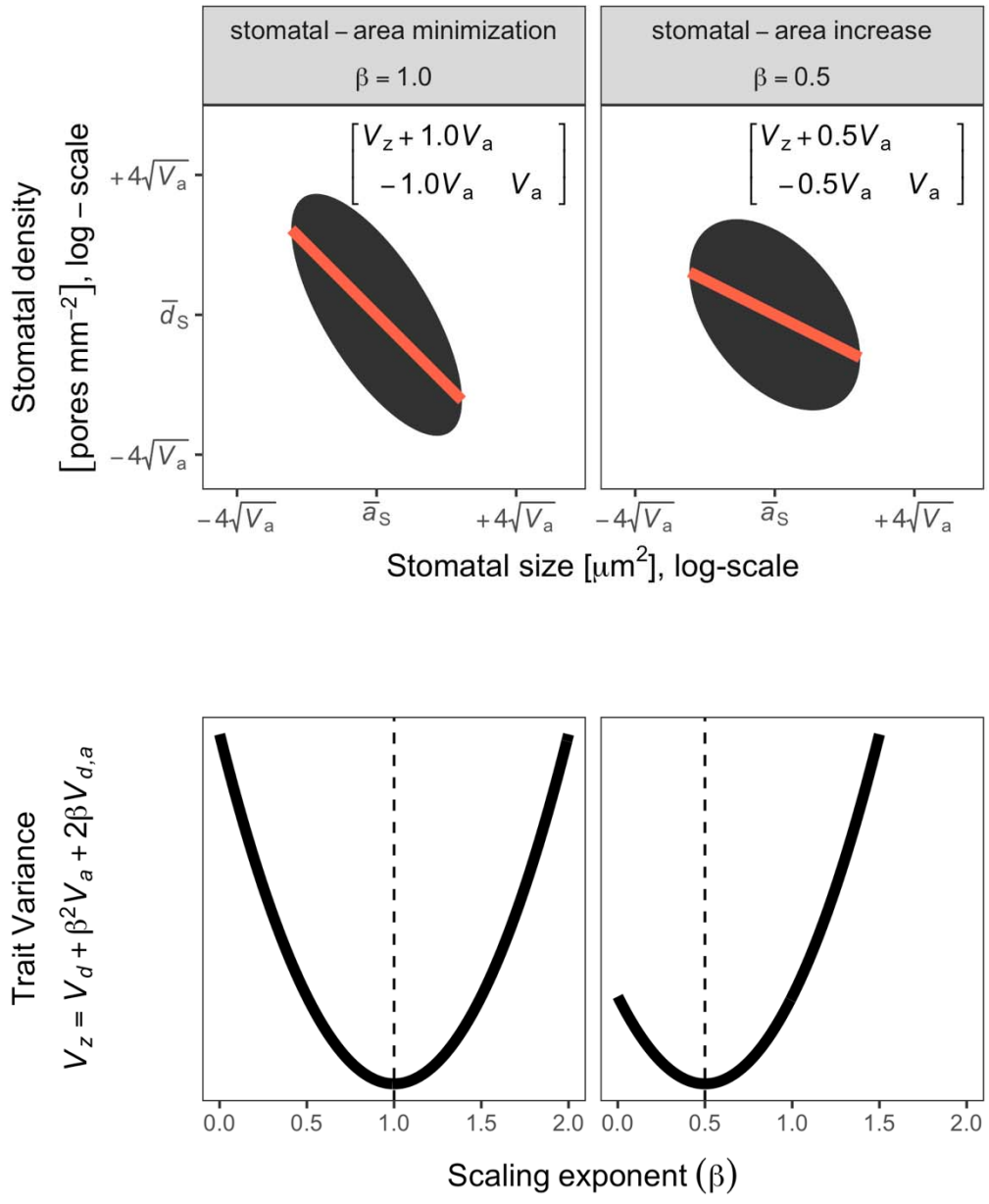

394

395 **Fig. 1 | Competing hypotheses for the origin of negative stomatal size-density scaling make**

396 **different predictions about the trait covariance structure.** Maximum stomatal conductance

397 (g_{max}) and the fraction of epidermal area allocated to stomata (f_S) are composite traits determined

398 by stomatal density and size. On a log-scale, they are the sum of log-stomatal density (d_S) and

399 log-stomatal size (a_S) times a scaling exponent (β), 0.5 for g_{max} and 1.0 for f_S (see Methods).
400 There are infinite number of other composite traits, which we denote z_S, associated with different
401 values of β (Eq. 4). **a.** A unique stomatal size-density covariance structure is associated with the
402 β that minimizes the variance in the resulting composite trait. If the means ($\bar{d}_S$, $\bar{a}_S$) and variances
403 (V_d, V_a) of stomatal density and size, respectively, can be measured, the covariance between
404 them ($V_{d,a}$) is equal to -βV_a. Under the stomatal-area increase (left panel) and stomatal-area
405 minimization (right panel) hypotheses, β should be 0.5 and 1, respectively. The ellipse is the
406 0.95 quantile of covariance ellipse associated with the covariance matrix (upper right corner of
407 the plot); the orange line is the scaling exponent fit through the constituent trait means. **b**. The
408 covariance structure depicted in **a** is that which minimizes the variance in a composite trait (V_z)
409 given a hypothesized scaling exponent.

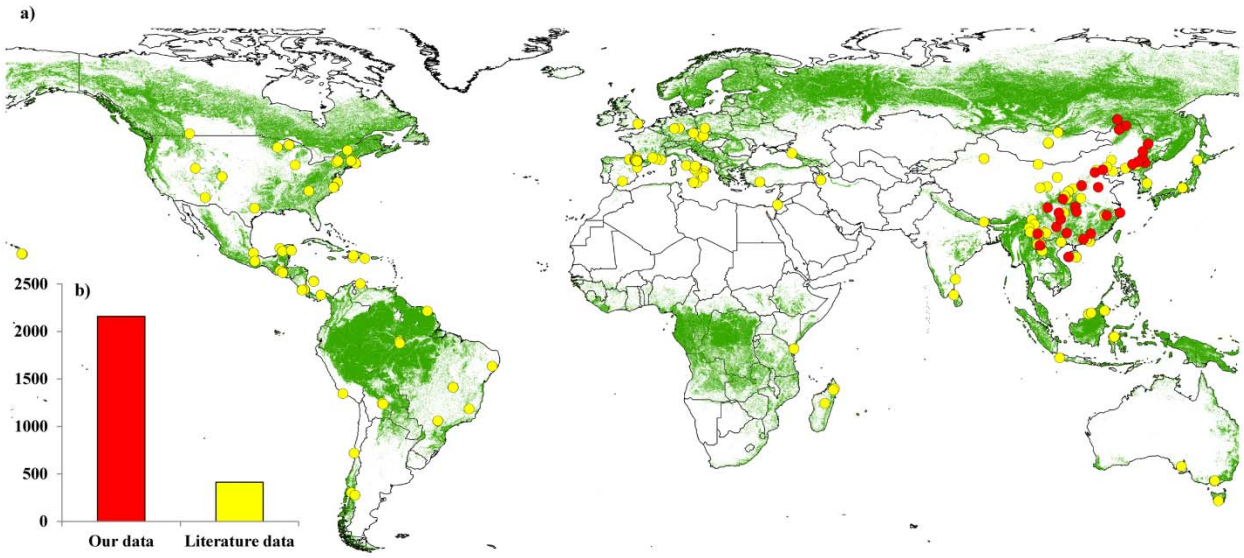

Fig. 2 | Geographic distribution of sampling sites (a) and the number of plant species (b) in this study.

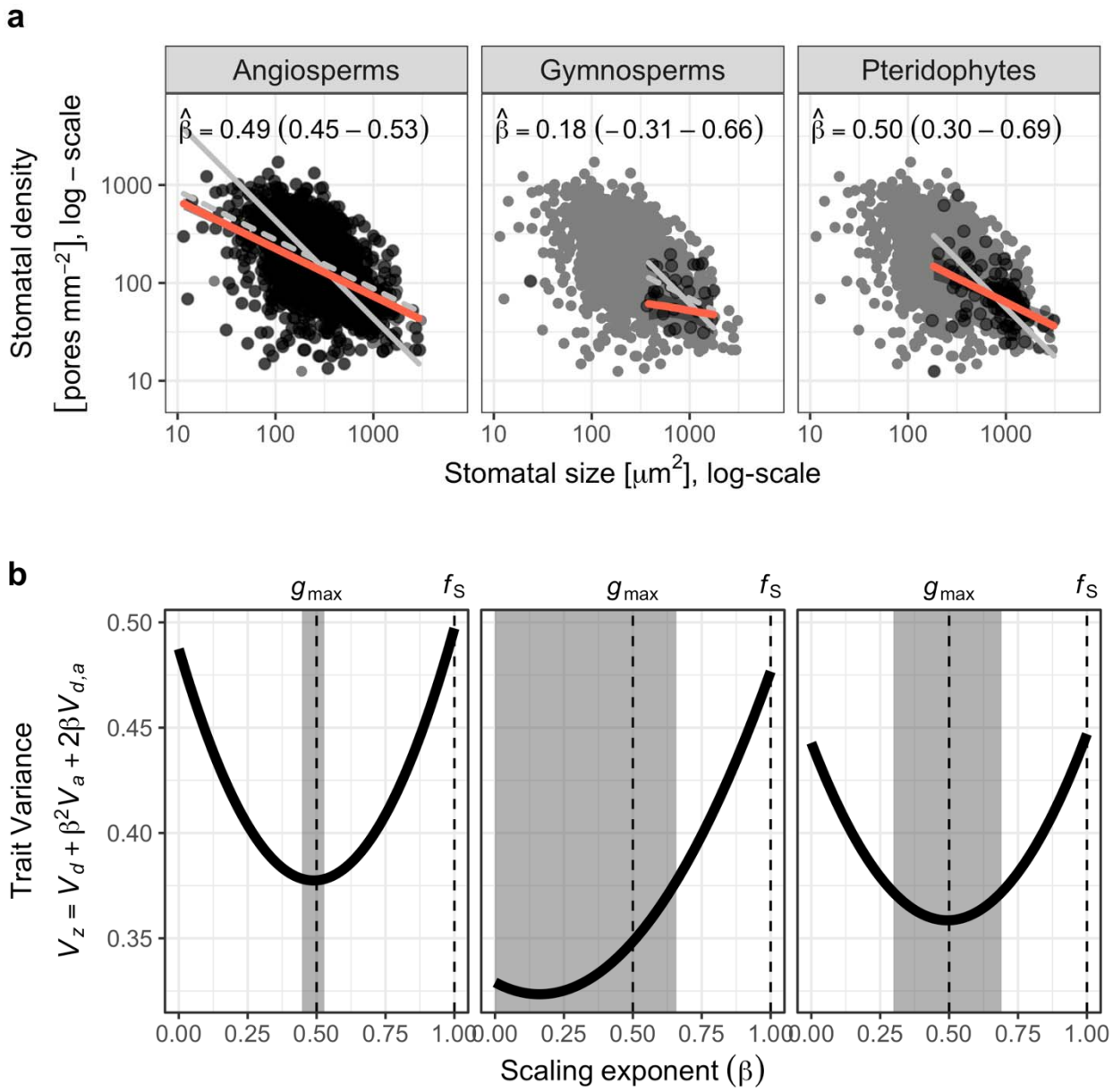

414

415 **Fig. 3 | Stomatal size-density scaling is consistent with stomata-area increase but not area-**

416 **minimization. a.** In both angiosperms (left panel) and pteridophytes (right panel), the scaling

417 exponent ( ) estimated as the phylogenetic linear regression slope of stomatal size against

418 density (Methods) is close to 0.5 as predicted by the stomatal-area increase hypothesis, but much

419 less than 1.0, as predicted by the stomatal-area minimization hypothesis. For comparison, thin

420 gray lines in the background show predicted slopes for each group when = 1.0 (solid line) and

421 β = 0.5 (dashed line). The bootstrap 95% confidence intervals are in parentheses and shown
422 graphically by the width of the grey rectangle in **b**. Dark points represent species mean trait
423 values from the focal group; grey background points are from all groups for comparison. Orange
424 line and ribbon are the estimated phylogenetic regression line and the 95% bootstrap confidence
425 intervals. Scaling in gymnosperms (middle panel) is not significantly different from 0 or 0.5, but
426 the confidence intervals do not include 1.0. **b.** The variance of the composite trait (V_z) is
427 minimized near β = 0.5, as predicted under the stomatal-area increase hypothesis (dashed-line
428 under g_{max}) but not where β = 1.0 as predicted by the stomatal-area minimization hypothesis
429 (dashed-line under f_S).

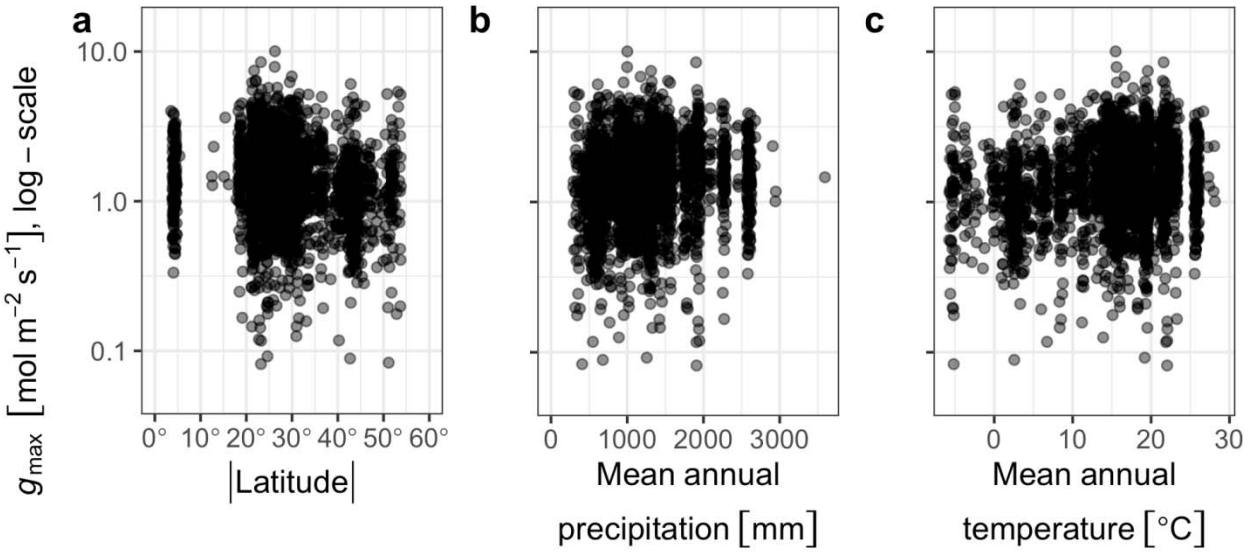

Fig. 4 | Anatomical maximum stomatal conductance varies little with latitude, mean annual precipitation, or mean annual temperature. Each point is the species' mean |latitude| (**a.**), mean annual precipitation (**b.**), or mean annual temperature (**c.**) on the *x*-axis and the maximum stomatal conductance (g_{max}) on the *y*-axis (log-scale).